WELDING OF HIGH-HARDNESS ARMOR STEEL

UDC:621.791.05:669.018.25
Original scientific paper https://doi.org/10.46793/adeletters.2022.1.4.5

Aleksandar Čabrilo[1*], Nenad Janjić[1]

[1] Higher Education Technical School of Professional Studies, Skolska 2, Novi Sad, Serbia

Abstract:
Armor steels are difficult to weld due to the high percentage of carbon. The coarse-grained area and the fusion line in the welded joint are sensitive areas due to the high hardness and the possible presence of hydrogen produced during the welding process. Furthermore, multi-purpose armored vehicles made of armored steel are exposed to dynamic loading due to traffic on rough terrain. High hardness in the coarse-grained area of the heat-affected zone and dynamic loading can cause cracks. In the weld metal zone, a crack created during the welding process or due to pores can quickly propagate toward the sensitive fusion line, after which its accelerated growth can occur. Based on the above, achieving a welded joint without porosity or cracks for armor steel is necessary. This paper investigated the welding process of high-hardness armor steel with two regimes. The test aims to achieve an optimal hardness level and a compromise between ballistic requirements and toughness. The test results showed that a high-quality welded joint and an optimal balance between hardness and toughness are achieved with increased heat input.

ARTICLE HISTORY
Received: 13.09.2022.
Accepted: 29.11.2022.
Available: 31.12.2022.

KEYWORDS
Armor steel, austenitic filler material, steel hardness, steel toughness, armored vehicles, GMAW process

1. INTRODUCTION

Multi-purpose armored vehicles are made of high-hardness armor steel [1,2]. Using high-hardness materials guarantees that armored vehicles will have better ballistic characteristics [3-5]. Due to its good properties at low temperatures, the austenitic filler material is used when welding armor steel [6]. Armored vehicles move over rough terrain during military operations, exposing them to dynamic loads. Armored vehicle materials show different behavior under dynamic load conditions than under static load conditions [7]. The coarse-grained region of the heat-affected zone (HAZ) is often very brittle due to high carbon content and hardness [8], which is why it is necessary to obtain an optimal balance between hardness and toughness [9,10]. In addition to HAZ, in the weld metal zone, possible pores and cracks result from an inadequate welding process [11]. The distance between possible pores in the weld metal and the fusion line is minimal. Therefore, obtaining a welded joint without cracks and pores is necessary.

Optimization of welding of armor steel is crucial [12,13]. When choosing the welding parameters, the preheating temperature, and the transition temperature, an analysis of the continuous cooling diagram (CCT diagram) is necessary. From the point of view of ballistic requirements and toughness of the welded joint, it is necessary to know the relationship between hardness and cooling rate.

The microstructure of the weld metal consists of an austenitic matrix with delta δ - ferrite. Delta ferrite does not allow the formation of a hot crack in the austenitic weld metal during the hardening process [14,15]. However, the presence of δ - ferrite results in lower hydrogen solubility and higher diffusivity, which can increase the tendency of the welded joint to hydrogen brittleness. Compared to other filler materials, the advantage of austenitic filler material is the slow diffusion of hydrogen through the austenite base [16,17], whereby

*CONTACT: Aleksandar Čabrilo, e-mail: cabrilo@vtsns.edu.rs

hydrogen diffuses more difficultly into the hard and brittle fusion line or coarse-grained region.

Due to the difference in composition, armor steels from different manufacturers have different CCT diagrams. Therefore, the choice of welding parameters and heat input will give different microstructures and hardness distributions for different armor steels.

2. MATERIALS AND METHODS

This study examined the welding process on the armor steel Protac 500. Similar tests regarding the armor steel Protac 500 were shown in research [18,19]. The chemical composition of the base and filler material is shown in Table 1 [1]. Spectrochemical analysis of the composition of the base and filler material after the welding process was obtained using the ARL 2460 device.

Table 1. Chemical composition of the base and filler material [1]

Material	*Chemical composition (mass fraction %)*										
	C	***Si***	***Mn***	***S***	***Cr***	***P***	***Al***	***Cu***	***Ni***	***Mo***	***V***
Protac 500	0,27	1,07	0,71	0,001	0,64	0,009	0,054	0,28	1,094	0,296	0,039
AWS ER307	0,08	0,89	6,29	0,001	17,8	0,014	0,01	0,08	8,24	0,13	0,03

Testing the welding process on armor steel was done with two welding regimes. When it comes to welding regime 1, the preparation of facing plates was done according to Fig.1, while for welding regime 2, it was done according to Fig.2. For both regimes, austenitic filler material is used. The welding direction is parallel to the rolling direction. Cold-rolled plates with a thickness of 12 mm were cut to the required dimensions (250 mm x 100 mm), while the V joint at the angle of 27.5 mm was prepared with a water jet cutting machine.

Welding parameters for the first regime are given in Table 2. Welding was performed in four passes. Root pass, filler passes, and cover passes are set for spray transfer. The welding was performed using the GMAW process in argon + 2.5% CO_2 protective atmosphere with a flow rate of 15 liters. The diameter of the wire is 1.0 mm.

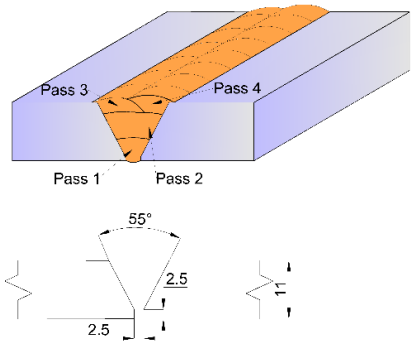

Fig. 1. Schematic representation of a welded joint and pass position for regime 1

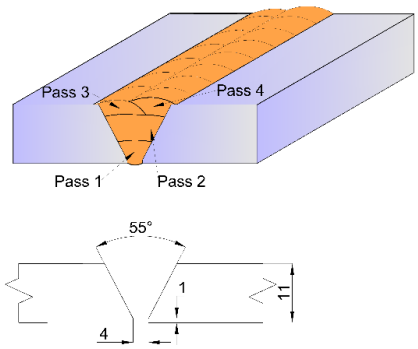

Fig. 2. Schematic representation of a welded joint and pass position for regime 2

The welding parameters for the second regime are given in Table 3. The parameters are set for short-circuit transfer for the root pass. The filler and cover passes are set for spray transfer. The GMAW process in argon+2.5 %CO_2 protective atmosphere with flux 10 x wire diameter and 12 x wire diameter for transfer in short circuit and spray, respectively. The diameter of the wire is 1.0 mm.

During the examination of the welding process with regime 1, a special device and a Fronius Time Synergic 450 welding machine were used. During the testing of the welding process with regime 2, the Kuka robot and the Citronix 400A GMAW machine were used. A special device and robot were used to eliminate the influence of human factors, then the possibility of fine-tuning the parameters of the welding process and the reproducibility of the results.

Table 2. Welding parameters and number of passes for multi-pass welding for regime 1

Pass	*Filler material*	*Preheating and interpass temperature* (° C)	*Heat input* (kJ/mm)	*Amperage* (A)	*Voltage* (V)	*Welding speed* (m/min)	*Wire speed* (m/min)	*Protect. atmosphere*
1	ER 307	120	0.98	275	26.7	0.45	-	Ar+ 2.5% CO_2
2		120	0.98	275	26.7	0.45	-	
3		120	0.98	275	26.7	0.45	-	
4		120	0.98	275	26.7	0.45	-	

Table 3. Welding parameters and number of passes for multi-pass welding for regime 2

Pass	*Filler material*	*Preheating and interpass temperature* (° C)	*Heat input* (kJ/mm)	*Amperage* (A)	*Voltage* (V)	*Welding speed* (m/min)	*Wire speed* (m/min)	*Protect. atmosphere*
1	ER 307	150	1,13	168	16.9	0.16	7.4	Ar+ 2.5% CO_2
2		160	2,13	215	25.5	0.15	12.9	
3		160	1,13	215	25.5	0.29	12.9	
4		160	1,13	215	25.5	0.29	12.9	

After the welding process, a radiographic examination was performed. For welding regime 1 (Table 2), a radiographic examination was performed on one pair of plates. At the same time, the radiographic examination of plates welded by regime 2 (Table 3) was performed on six pairs of plates.

The amount of δ - ferrite in the austenite base was determined with a ferritoscope device. The mass fraction of magnetic ferrite was measured with a ferritoscope in the root of the weld metal - the lower part of the weld metal, then in the filling zone - the middle of the weld metal, as well as in the covering passes in the upper part of the weld metal.

A metallographic examination of the welded joint was performed by cutting the sample and placing it in epoxy resin. Next, the sample was grindend with abrasive paper and polished with diamond paste. After that, the sample was etched using 2% Nital. Finally, analysis of the microstructure of the welded joint of armor steel was done with an SEM microscope JEOL JSM 6460LV.

In order to characterize the welded joint, it was necessary to test the hardness. The welded joint should have a hardness that is in accordance with the standard MIL-STAN-1189. The hardness test was done 2 mm below the top surface, then in the weld metal in the middle. Hardness tests were also done along the fusion line since achieving optimal values in this critical zone is essential. A Digital Micro Vickers Hardness Tester HVS1000, Laiznou Huayin Testing Instrument Co, was used for micro-hardness testing, with a load of 500 gr.

Testing the tensile characteristics was done in accordance with the EN 895 standard. A water jet cutting machine was used for the rough cutting of the test sample. In addition, a waterjet cutting machine was used to eliminate the possibility of thermal effects on armor steel. Testing the tensile characteristics was performed on the Instron 8033 servo-hydraulic shear. The deformation rate is 0.125 mm/sec.

3. RESULTS AND DISCUSSIONS

3.1 Results of radiography

According to the radiography results, joints welded with regime 1 have high porosity. Porosity is present in every pass. The size of the largest pore is 1.5 mm. Cracks are not present in the welded joint. According to regime 2, the welded joint has no porosity or crack, and the welded joint is rated with the highest class B.

3.2 Results of microstructure and hardness

The appearance of a welded pair of plates according to regimes 1 and 2 are given in Fig.3 and 4, respectively. In Fig.3, the pores are visible in each of the four passes, while in Fig.4, there are no pores.

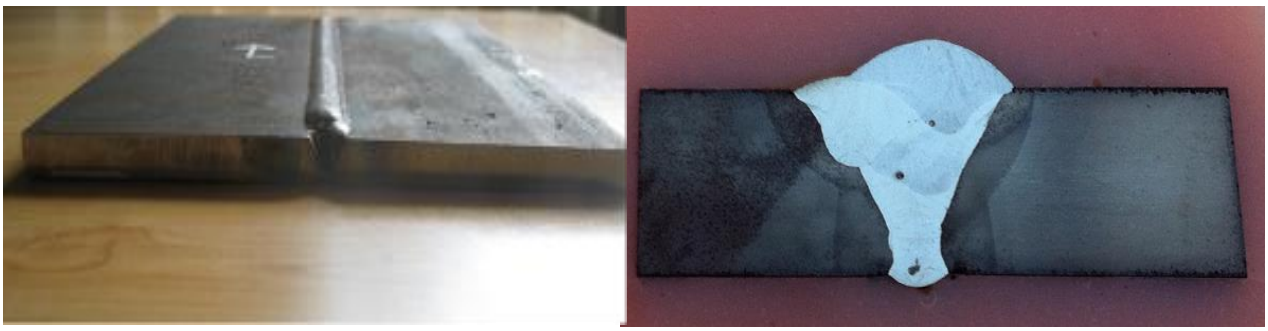

Fig. 3. Welded plates using the welding regime 1

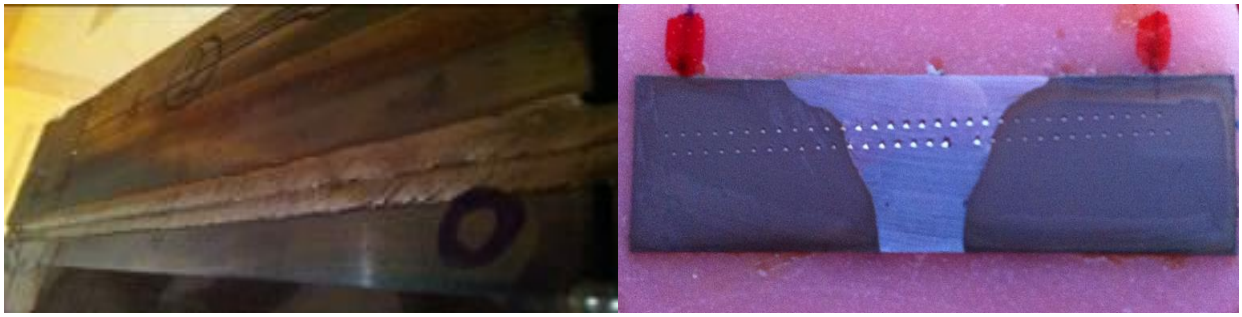

Fig.4. Welded plates using the welding regime 2

The microstructure test was performed on samples welded with welding regime 2. The microstructure of the weld metal in Fig.5 a) and d) consists of an austenite base and δ ferrite. The amount of δ-ferrite measured with a ferritoscope at the root of the weld metal is 11.7 %mass. In the middle of the weld metal, it is 5.4 %mass, while in the upper part, 3.2 %mass. The coarse-grained region of HAZ, Fig.5 b) and e), shows the microstructure of upper and lower bainite and martensite. The fine-grained area of Fig. 5 c) and f) consists of a mixture of upper and lower bainite.

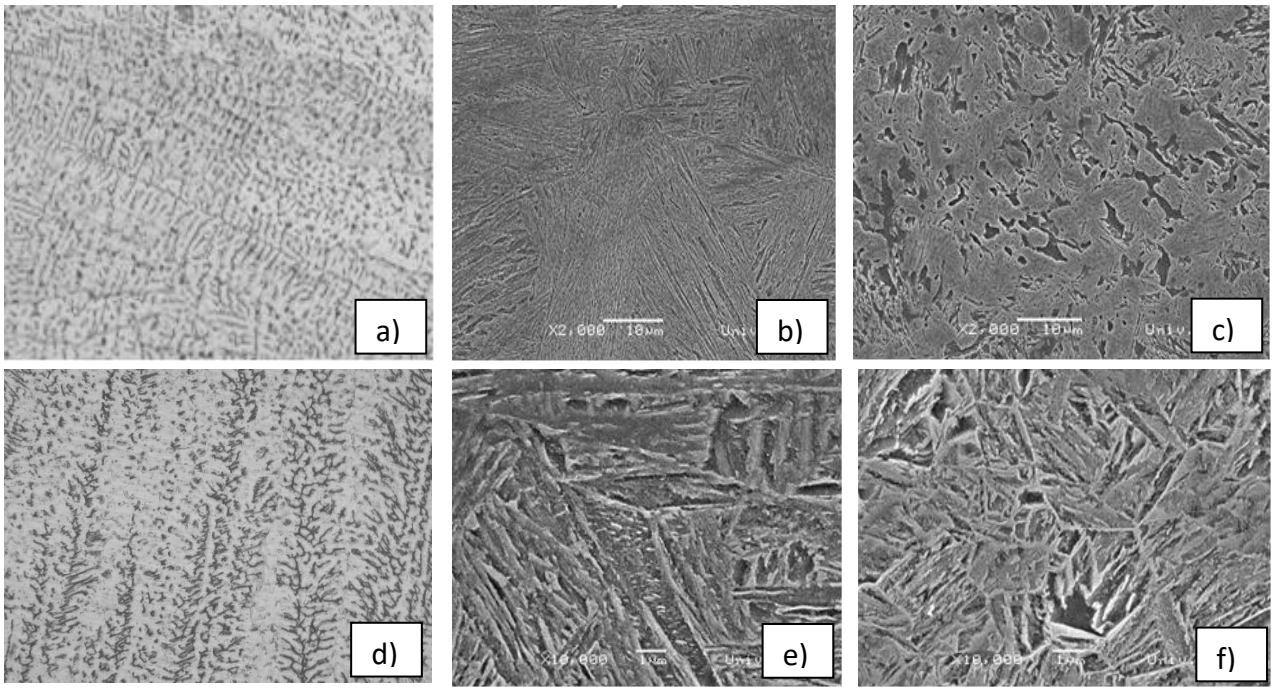

Fig. 5. Microstructure of the welded joint of armor steel using the welding regime 2: a) and d) weld metal, b) and e) coarse-grained HAZ, c) and f) fine-grained HAZ

Fig.6 and 7 show the change in hardness 2 mm below the top surface in the zones: weld metal, fusion line, HAZ, and base metal, for regimes 1 and 2, respectively. The hardness in the weld metal zone for regime 1 is between 250 HV and 370 HV. On the other hand, regarding regime 2, the hardness in the weld metal zone is between 190 HV and 350 HV. The hardness increases from the middle of the weld metal, where the value is 190 HV, while along the fusion line on the side of the weld metal, the value is 350 HV. The hardness at the fusion line is 420 HV and 425 HV for regimes 1 and 2, respectively.

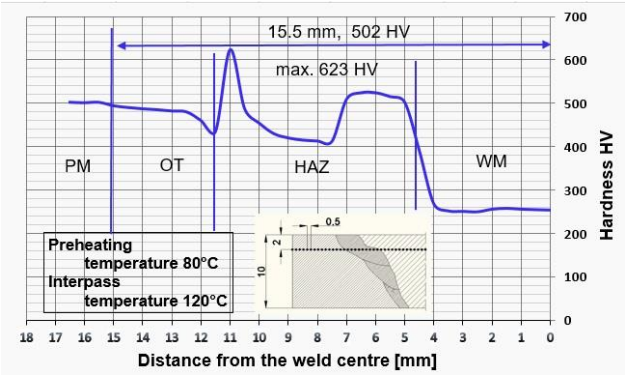

Fig. 6. Weld joint hardness profile for regime 1 measured 2 mm below the top surface. *(Note: WM-weld metal, HAZ-heat-affected zone, IC-inter-critical zone, SC-sub-critical zone, and PM-base metal)*

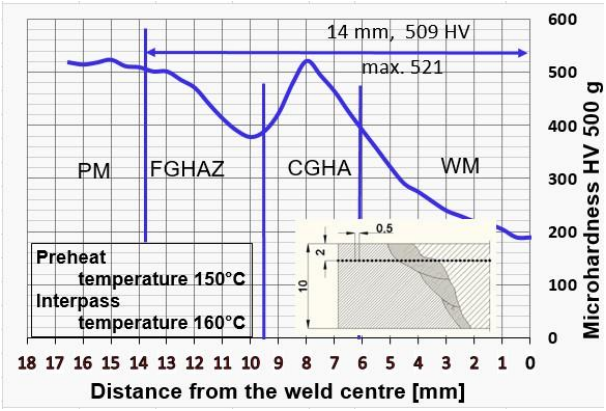

Fig. 7. Weld joint hardness profile for regime 2 measured 2 mm below the top surface. *(Napomena: WM-weld metal, HAZ-heat-affected zone, IC-inter-critical zone, SC-sub-critical zone, and PM-base metal)*

Regarding the HAZ, maximum hardness is in the coarse-grained region for both regimes. The maximum hardness is 623 HV and 521 HV for regimes 1 and 2, respectively. The hardness trend for regime 2 increases and reaches a maximum value of 521 HV at a distance of 8 mm from the weld metal axis. After the maximum for both regimes, the hardness trend decreases, reaching a minimum value of 430 HV at a distance of 11.7 mm and 378 HV at a distance of 10 mm from the weld axis for regimes 1 and 2, respectively. At a distance of 15.5 mm and 14 mm from the weld metal axis, the hardness value is approximately 509 HV for both regimes, which corresponds to the hardness of the base metal.

More detailed examinations of the hardness distribution were continued with the samples welded with regime 2. The goal of continuing the hardness measurement in the middle of the weld metal zone in Fig.8, with regime 2, is to determine the level of mixing of the base and filler material. The hardness values are between 190 HV and 225 HV. The maximum hardness is 225 HV in the narrow zone, while the lower values are 190 HV in the broader weld metal zone. The change in the hardness trend is the mixing of the base and filler material, and it is more intense in the narrow zone, while in the broader zone, mixing almost does not occur. For regime 2, the hardness was measured along the zone following the fusion line. The width of the zone is 0.5 mm, Fig.9. The results show that the hardness along the fusion line does not exceed 442 HV. The hardness values are between 418 HV and 442 HV. The hardness trend decreases with decreasing height. It is a minimum of 412 HV in the upper zone and a maximum of 422 HV in the lower zone. The heat effect is more significant in the zones closer to the rear passage than in the further zones, which must have been influenced by the already cooled filler and base material.

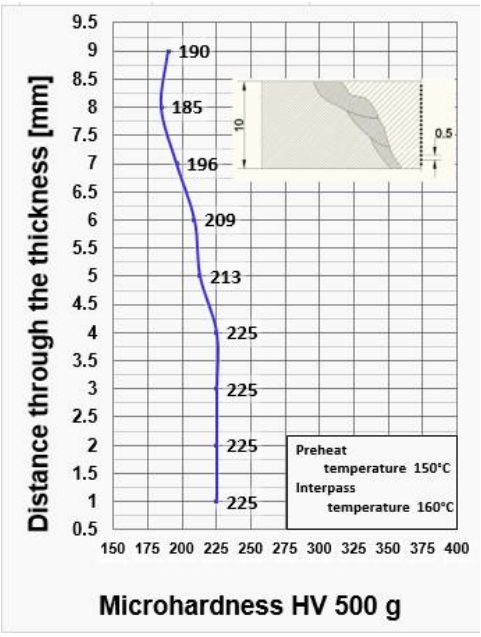

Fig. 8. Hardness distribution in the middle of the weld metal using regime 2

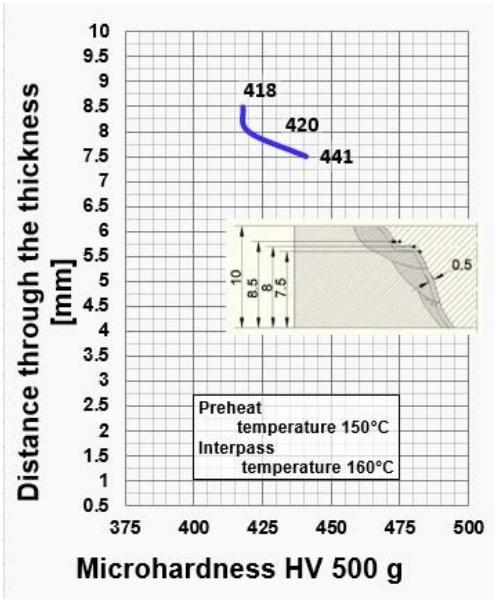

Fig. 9. Hardness distribution along the fusion line using regime 2

3.3 Results of tensile properties

The results regarding the tensile properties for regime 2 are shown in Table 4. A high tensile strength of 833 MPa is noticeable, while the yield stress is within the expected limits of 552 MPa. The difference between tensile strength and yield stress is 281 MPa.

Table 4. Tensile properties for four-pass GMAW process using austenite filler material

Sample no.	Tensile strength (MPa)	Yield strength (MPa)
1	825	589
2	833	552

A preheating temperature of 150°C and an interpass temperature of 160°C for regime 2 enabled slower cooling in the temperature interval from 600°C to 200°C, compared to a preheating temperature of 120°C and an interpass temperature of 120°C for regime 1. The preheating and interpass temperatures gave adequate hardness to the coarse-grained region of HAZ. The cooling rate enabled slow cooling and obtaining softer phases in the coarse-grained region of HAZ, which is in accordance with the CCT diagram [20]. A martensitic-bainite structure is obtained from the same diagram for these cooling rates.

The protective atmosphere in the Ar+2.5 CO2 mixture provided adequate protection during the welding process.

When it comes to hardness values for welding regimes 1 and 2, hardness higher than 509 HB was achieved at a distance of 15.5 and 14 mm for regimes 1 and 2, respectively. Both regimes met the requirement of the MIL-STAN-1185 [21] standard clause that the hardness must not fall below 509 HV at a distance of 15.9 mm from the weld metal. However, regime 1 is very close to this value. The maximum hardness in the coarse-grained region of HAZ is 623 HV and 521 HV for regimes 1 and 2, respectively. The hardness of 623 HV is very high, where even a tiny amount of hydrogen present in this zone can create cracks. With a hardness of 521 HV, for regime 2, in the coarse-grained region of HAZ, a good balance between ballistic protection on the one hand and toughness on the other was achieved. With a hardness of 521 HV, a larger allowed amount of hydrogen in the coarse-grained region of HAZ is enabled, and it amounts to 1÷5 ml per 100 grams of weld metal.

4. CONCLUSION

This work examined the weldability of high-hardness armor steel with two different regimes. The test aimed to achieve optimal hardness and meet the MIL-STAN-1185 standard. In order to see the broader picture of the welded joint, the microstructure, hardness, and tensile properties were analyzed. Based on the results, the following conclusions can be drawn:

- Regime 1 and plate preparation with this regime produced a welded joint with high porosity. With regime 2, a welded joint without porosity and cracks was obtained, while the welded joint was rated as class B. The repeatability of the results was obtained on six welded joints;
- For regime 2, the difference in tensile strength (833 MPa) and yield stress (552 MPa) of 281 MPa results in good ductility of the welded joint;
- The optimal balance between hardness and toughness was achieved by regime 2. Regime 1 achieved a maximum hardness of 623 HV, which is unacceptable due to its tendency to crack;
- The MIL-STAN-1185 standard is met with both welding regimes. However, regime 1, with the width of the changed zone of 15.5 mm from the axis of the weld metal, is at the limit of acceptability.

REFERENCES

[1] B. Savic, A. Cabrilo, Effect of Heat Input on the Ballistic Performance of Armor Steel Weldments. *Materials*, 14(13), 2021: 3617. https://doi.org/10.3390/ma14133617

[2] Y.H. Cheng, H. Wu, R.G. Zhao, F. Zhou, Mechanical characteristics and ballistic behaviors of high strength and hardness armor steels. *Journal of Constructional Steel Research*, 197, 2022: 107502. https://doi.org/10.1016/j.jcsr.2022.107502

[3] Z. Fei, Z. Pan, D. Cuiuri, H. Li, A.A. Gazder, A Combination of Keyhole GTAW with a Trapezoidal Interlayer: A New Insight into Armour Steel Welding. *Materials*, 12(21): 3571. https://doi.org/10.3390/ma12213571

[4] G. Magudeeswaran, V. Balasubramanian, G. Madhusudan Reddy, Metallurgical characteristics of armour steel welded joints used for combat vehicle construction. *Defence Technology*, 14(5), 2018: 590-606. https://doi.org/10.1016/j.dt.2018.07.021

[5] M.A. Morsy, S.M. Abdel Aziz, K. Abdelwahed, S.A. Abdelwahab, Effect of welding parameters on the mechanical and metallurgical properties of armor steel weldment. *Journal of Engineering and Applied Science*, 69, 2022: 62. https://doi.org/10.1186/s44147-022-00102-7

[6] N.M. Stanković, S.T.M. Vulović, Z.Z. Adamović, A.L.N. Ašonja, M.S. Vulović, The model of five states and its implementations to reliability and steam turbines. *Journal of the Balkan Tribological Association,* 23(3), 2017: 542-568.

[7] D. Lenihan, W. Ronan, P.E. O'Donoghue, S.B. Leen, A review of the integrity of metallic vehicle armour to projectile attack. *Proceedings of the Institution of Mechanical Engineers, Part L: Journal of Materials: Design and Applications*. 233(1), 2019: 73-94. https://doi.org/10.1177/1464420718759704

[8] A. Cabrilo, A. Sedmak, Z. Burzic, S. Perkovic, Fracture mechanics and fatigue crack propagation in armor steel welds. *Engineering Failure Analysis,* 106, 2019: 104155. https://doi.org/10.1016/j.engfailanal.2019.104155

[9] E. Konca, A Comparison of the Ballistic Performances of Various Microstructures in MIL-A-12560 Armor Steel. *Metals*, 10(4), 2020: 446. https://doi.org/10.3390/met10040446

[10] A. Popławski, P. Kędzierski, A. Morka, Identification of Armox 500T steel failure properties in the modeling of perforation problems. *Materials & Design*, 190, 2020: 108536. https://doi.org/10.1016/j.matdes.2020.108536

[11] A. Cabrilo, K. Geric, O. Klisuric, M. Cvetinov, Toughness Behaviour in Armour Steel Welds. *Tehnički vjesnik,* 25(6), 2018: 1699-1707. https://doi.org/10.17559/TV-20170722201539

[12] J. Youngcheol, K. Chankyu, L. Seungjun, J. Yongmun, P. Choulsoo, L. Byungsuk, P. Taewon, K. Hongkyu, C. Young Tae. Welding Technical Trend of High Hardness Armour Steel for Combat Vehicle. *Journal of the Korea Institute of Military Science and Technology,* 22(3), 2019: 299-310. https://doi.org/10.9766/KIMST.2019.22.3.299

[13] I. Garašić, M. Jurica, D. Iljkić, A. Barišić, Determination of ballistic properties on armox 500T steel welded joint. *Engineering Review*, 39(2), 2019: 186-196. http://doi.org/10.30765/er.39.2.8

[14] T. Michler, J. Naumann, Microstructural aspects upon hydrogen environment embrittlement of various bcc steels. *International Journal of Hydrogen Energy*, 35(2), 2010: 821-832. https://doi.org/10.1016/j.ijhydene.2009.10.092

[15] Y. Mine, C. Narazaki, C. Murakami, S. Matsuok, Y. Murakami, Hydrogen transport in solution treated and pre-strained austenitic stainless steels and its role in hydrogen-enhanced fatigue crack growth. *International Journal of Hydrogen Energy*, 34(2), 2009: 1097-1107. https://doi.org/10.1016/j.ijhydene.2008.11.018

[16] L. Kuzmikova, J. Norrish, H. Li, M. Callaghan, Research to establish a systematic approach to safe welding procedure development using austenitic filler material for fabrication of high strength steel, *16th International Conference on the Joining of Materials,* Faculty of

engineering and information sciences - papers: part A, Australia, 2011, pp.1-13.

[17] L. Kuzmikova, An investigation of the weldability of high hardness armour steels, Ph. D. thesis. *Faculty of engineering*, *University of Wollongong*, Australia, 2013.

[18] J. Bernetič, B. Kosec, G. Kosec, M. Gojić, Z. Burzić, A. Nagode, M. Soković, M. Bizjak, A new generation of armored steel plates. *Contemporary Materials*, 7(2), 2016: 137-141. https://doi.org/10.7251/COMEN1602137B

[19] J. Trajkovski, R. Kunc, V. Pepel, I. Prebil, Flow and fracture behavior of high-strength armor steel PROTAC 500. *Materials & Design*, 66(Part A), 2015: 37-45. https://doi.org/10.1016/j.matdes.2014.10.030

[20] J. Bernetič, Development of model for predicting hardenability of high strength low alloy steels, Ph. D. thesis. *University Ljubljana*, Slovenia, 2013.

[21] Standard MIL-STD-1185, Department of defense manufacturing process standard: welding, high hardness armor, 2008. (SUPERSEDES MIL-W-62162).